Carrier Lifetime Stability of Boron-Doped Czochralski-Grown Silicon Materials for Years After Regeneration in an Industrial Belt Furnace

Lailah Helmich, Dominic C. Walter, Thomas Pernau, and Jan Schmidt

***Abstract*—We examine the long-term stability of the carrier lifetime in boron-doped Czochralski-grown silicon materials with different boron and oxygen concentrations, which were regenerated in an industrial belt furnace. After firing and subsequent regeneration in an industrial conveyor-belt furnace, the silicon samples are exposed to long-term illumination at an intensity of 0.1 suns and a sample temperature of about 30 °C for more than two years. After regeneration, we observe a minor re-degradation (30–72% reduced compared to the degradation observed without regeneration step). We attribute this re-degradation to a non-completed regeneration within the belt furnace due to the short regeneration period. Our results show that the industrial process consisting of firing with subsequent regeneration in the same unit is very effective for industrially relevant silicon materials. Typical industrial silicon wafers with a resistivity of (1.75 ± 0.03) Ωcm and an interstitial oxygen concentration of (6.9 ± 0.3) × 10^{17} cm^{-3} show lifetimes larger than 2 ms after regeneration and two years of light exposure.**

***Index Terms*—Boron–oxygen (BO) defect, carrier lifetime, Czochralski-grown silicon (Cz-Si), light-induced degradation (LID), long-term stability, regeneration.**

I. Introduction

IN BORON-DOPED Czochralski-grown silicon (Cz-Si), the carrier lifetime degrades severely under illumination near room temperature due to the activation of a boron–oxygen (BO) defect center [1]–[3]. A brief anneal in the dark at increased temperatures (e.g., 200 °C) was found to deactivate the BO center [1], however, this deactivation is not permanent and illumination at room temperature leads again to the full activation of the BO defect. If the samples are, however, illuminated during the annealing, it was found that the BO defect can be permanently deactivated [4]. This permanent BO deactivation process, which is accompanied by a permanent regeneration of the carrier lifetime, is triggered by the presence of excess carriers and not by photons. Hence, the regeneration process was found to depend critically on the illumination intensity [5]. In addition, it depends on the detailed thermal pre-treatment [6] of the sample. By the permanent deactivation of the BO defect, the efficiency of solar cells based on p-type boron-doped Cz-Si can be improved by up to 3% absolute [7], [8].

In this contribution, commercially available boron-doped, p-type Cz-Si wafers from different manufacturers are regenerated in an industrial belt furnace as already beneficially used in [9] for solar cells. The long-term stability of the carrier lifetime is examined over more than two years of illumination at an intensity of 0.1 suns. Our experiments clearly demonstrate the benefits of adding the regeneration step to lifetime samples, which underwent an industrial cell process sequence.

TABLE I
Resistivities ρ and Interstitial Oxygen (O_i) Concentrations of the Investigated Boron-Doped Cz-Si Materials of Various Manufacturers

Material	Resistivity [Ωcm]	O_i concentration [$\times 10^{17}$ cm^{-3}]	
		Center	Corner
A	1.75±0.03	6.9±0.3	7.1±0.5
B	1.76±0.02	7.7±0.5	8.3±0.1
C	1.08±0.09	8.4±0.2	6.8±0.2
D-1	1.73±0.02	10.5±0.7	9.6±0.3

The ρ values are obtained from 4-point-probe measurements and the O_i concentrations from FTIR measurements.

II. Experimental Details

We examine four different boron-doped Cz-Si materials with different boron and oxygen concentrations (see Table I) originating from various manufacturers. As a reference, boron-doped Fz-Si material is also included in the experiment. Whereas materials A and B in Table I are typical present-day industrial Cz-Si materials with homogeneously distributed oxygen concentrations over the wafer (center and corner), material C is a standard Cz-Si material from the early 2000s with a relatively inhomogeneously distributed oxygen concentration. Material D is stemming from the top region of a silicon crystal (seed end). According to the manufacturer's data, wafers from different heights of this seed end have the same oxygen concentration, so we investigate material D-1 representatively for the three

Manuscript received July 7, 2021; revised August 27, 2021; accepted September 21, 2021. Date of publication October 26, 2021; date of current version December 23, 2021. This work was supported in part by the German State of Lower Saxony and in part by the German Federal Ministry of Economics and Energy within the research project "Upgrade Si-PV" under Contract 0325877B. *(Corresponding author: Lailah Helmich.)*

Lailah Helmich and Jan Schmidt are with the Department of Solar Energy, Institute of Solid State Physics, Leibniz University of Hannover, D-30167 Hannover, Germany, and also with the Institute for Solar Energy Research Hamelin, D-31860 Emmerthal, Germany (e-mail: l.helmich@isfh.de; j.schmidt@isfh.de).

Dominic C. Walter is with the Institute for Solar Energy Research Hamelin, D-31860 Emmerthal, Germany (e-mail: d.walter@isfh.de).

Thomas Pernau is with the Centrotherm International AG, D-89143 Blaubeuren, Germany (e-mail: thomas.pernau@centrotherm.de).

Color versions of one or more figures in this article are available at https://doi.org/10.1109/JPHOTOV.2021.3116019.

Digital Object Identifier 10.1109/JPHOTOV.2021.3116019

different heights in the following. The oxygen concentrations are determined via Fourier transform infrared (FTIR) spectroscopy using a *VERTEX 70* (Bruker) FTIR spectrometer. As calibration factor $K = 3.14 \times 10^{17}$ cm^{-1} is used according to the IOC88 standard.

All wafers undergo a phosphorus diffusion step using $POCl_3$ in a quartz tube furnace (∼830 °C, 3 h). Afterward, the resulting phosphosilicate glass layers and the n^+-regions on both wafer surfaces are removed by hydrofluoric acid and potassium hydroxide solution. The final wafer thickness of all materials amounts to (164 ± 10) µm (error refers to the wafer-to-wafer scattering) to ensure comparability. Both surfaces of each wafer are passivated using aluminum oxide (Al_2O_3)/silicon nitride (SiN_x) stacks. The Al_2O_3 (10 nm) is deposited via plasma-assisted atomic layer deposition (PA-ALD) in a FlexAl system from Oxford Instruments and the SiN_x (70 nm) via plasma-enhanced chemical vapor deposition (PECVD) in a SiNA system from Meyer Burger Technology AG. The SiN_x layer has a refractive index of $n = 2.05$ as determined by ellipsometry at a wavelength of 633 nm. An RCA cleaning sequence is applied before each process step.

The lifetime samples, Fz- and Cz-Si wafers, are then submitted to a combined firing-regeneration process in an industrial infrared conveyor-belt furnace of type *c.FIRE.REG* 9600 from Centrotherm International AG [10]. For the regeneration treatment, we choose a regeneration temperature of 232 °C (measured) and an illumination intensity (of 7–9 suns). In addition, lifetime samples made of the same p-type Cz-Si materials and, in addition, Fz-Si lifetime samples are just fast-fired without the subsequent regeneration process in the industrial infrared conveyor-belt furnace DO-FF-8.600-300 from Centrotherm International AG with an adapted firing profile (set temperature $\vartheta_{\mathrm{set}} = 850\,^{\circ}\mathrm{C}$) according to the temperature treatment in the *c.FIRE REG*. For the combined firing-regeneration treatment, we choose a profile as illustrated in [10], green curve, but higher measured peak temperatures. Lifetime samples were processed equivalent to the blue curve in [10].

After firing, all lifetime samples are illuminated at room temperature (sample temperature ∼30 °C) at an illumination intensity of $I_{\mathrm{ill}} = 0.1$ suns (10 mW/cm^2) using halogen lamps. The illumination intensity is adjusted to the equivalent generated current density of the sun's spectrum using a calibrated reference silicon solar cell. In between the periods of illumination, the lifetime is measured in the center of the samples using a WCT-120 lifetime tester from Sinton Instruments [11]. If not stated otherwise, carrier lifetimes are reported at an excess carrier concentration of $\Delta n = 10^{15}$ cm^{-3} with a relative uncertainty of 10% [12]. Photoconductance decay (PCD) measurements are taken in the center of the lifetime samples if not mentioned otherwise. In addition, spatially resolved lifetime measurements are performed by applying the photoconductance-calibrated photoluminescence lifetime imaging (PC-PLI) technique [13]. The lifetime samples on which the regeneration process was omitted are annealed in darkness at 200 °C on a hotplate for 10 min prior to light exposure [see $t_{\mathrm{ill}} = 0$ h in Fig. 1(a)] to determine the BO-related lifetime limitations. The industrially

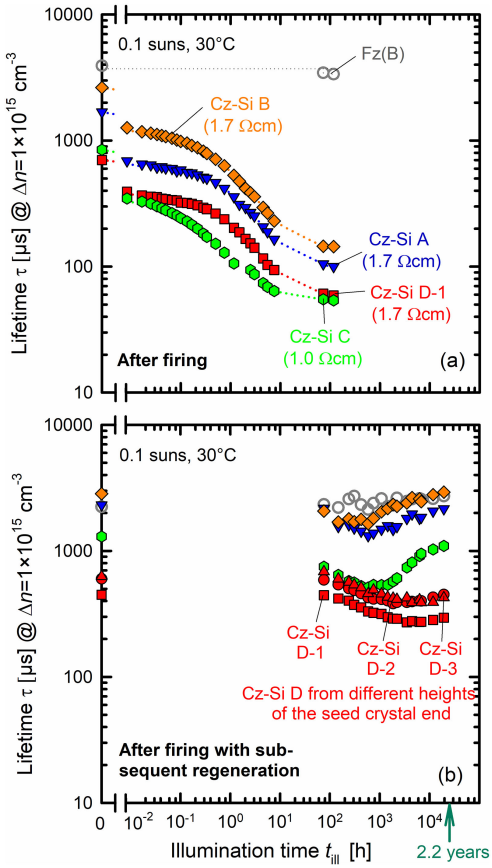

Fig. 1. Lifetime evolution of p-type Cz-Si materials A, B, C, and D from different manufacturers (filled symbols) and an Fz reference sample (open symbols) under illumination at 0.1 suns at 30 °C (a) after firing in an industrial belt furnace and (b) after firing with subsequent regeneration in an industrial belt furnace.

regenerated samples are illuminated for more than two years to examine the long-term lifetime stability after industrial regeneration.

III. Lifetime Stability After Regeneration in an Industrial Belt Furnace

Fig. 1 shows the evolution of the carrier lifetime during illumination at 0.1 suns as a function of the illumination time at room temperature for the materials A–D as well as for the reference Fz-Si material (ρ = 1.2 Ωcm). Fig. 1(a) includes the samples that were just fired in the industrial belt furnace and Fig. 1(b) shows the samples that were fired and subsequently regenerated in the *c.FIRE REG* furnace. Lifetime samples of materials A–C reach at least as high lifetimes (in the range of milliseconds) after firing and subsequent regeneration as directly after firing and dark annealing. The dark annealing step is necessary to temporarily deactivate the BO defect. The lifetime of material D is only 450 µs after firing and subsequent regeneration, which is significantly lower than the lifetime measured after firing and dark annealing, which amounts to 700 µs. This finding might indicate that additional background defects are present in material D after the regeneration treatment. The lifetime of the only-fired lifetime samples of all Cz-Si materials degrades

by ∼90% (fully activated BO defect) in relation to the lifetime after 10 min of annealing at 200 °C in the dark [temporarily deactivated BO defect, see $t_{\mathrm{ill}} = 0$ h in Fig. 1(a)]. In detail, material A degrades from 1690 µs to 100 µs, material B from 2630 µs to 150 µs, material C from 850 µs to 50 µs, and material D-1 from 700 µs to 60 µs. From the measured lifetimes $\tau(t)$ evolution and the lifetime measured directly after dark annealing τ_0, the effective defect concentration $N_t^* = 1/\tau(t) - 1/\tau_0$ can be determined.

The time evolution of N_t^* during light-induced degradation can be described by an exponential function with a degradation rate constant R_{deg}. The determined R_{deg} values of the only-fired samples amount to 3.1×10^{-5} s^{-1} for materials A and D (lower doping concentration) and 1.2×10^{-4} s^{-1} for material C (higher doping concentration). These values are in agreement with the defect generation rate constants of the light-induced BO defect activation published in the literature [14], for unfired samples of the same doping concentrations. According to [14], the defect generation rate constant does not depend on the oxygen concentration. Obviously, the firing step has no influence on the degradation rate constants as well.

PCD and PC-PLI measurements of the fired and subsequently regenerated Cz-Si wafers are shown in Figs. 1(b) and 3. The lifetime after the permanent deactivation of the BO defect initially decreases under illumination at room temperature. Only the lifetime of the p-type Fz-Si reference sample is fully stable over the entire period of illumination, which indicates that the surface passivation is stable under these conditions. In addition, we calculated the time-resolved saturation current density J_0 for all samples [15]. The J_0 values (not shown here) are stable within the scattering, which supports the statement that the surface passivation quality stays stable during illumination.

Lifetime samples made of materials A and B, which are fired and subsequently regenerated, degrade in the first 587 h of illumination with a degradation rate constant of $R_{\mathrm{deg}} = 9.7 \times 10^{-7}$ s^{-1}, whereas lifetime samples of material C reach a minimum in lifetime after 751 h of illumination with $R_{\mathrm{deg}} = 2.2 \times 10^{-6}$ s^{-1}. A similar degradation behavior was already reported in the literature [16] for the same material regenerated on a hotplate. Lifetime samples of material D degrade even longer/slower (3517 h) with $R_{\mathrm{deg}} = 3.6 \times 10^{-7}$ s^{-1}. These degradation rate constants are much lower than the typical BO degradation rates without any regeneration treatment applied. The degradation rate constants are reduced by up to two orders of magnitude due to the regeneration treatment. In addition, the degradation extent is significantly reduced after regeneration compared to the lifetime samples, which only underwent the firing step without regeneration. The subsequent industrial regeneration reduces the subsequent lifetime degradation by at least 30% (material D) and in the best case by 72% (material A). The samples made from material D degrade after regeneration only to 270 µs compared to 60 µs for the only-fired case. Samples made from material A degrade only to 1320 µs after regeneration instead of 110 µs for the only-fired case. Hence, the samples show a significantly improved lifetime stability by firing with a subsequent regeneration step compared to without the regeneration step.

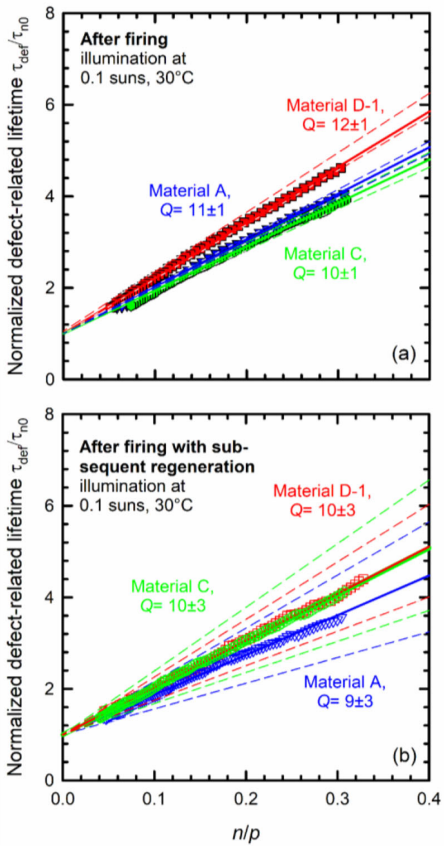

Fig. 2. Normalized defect-related lifetime $\tau_{\mathrm{def}}/\tau_{\mathrm{n0}}$ of the light-induced defect for fired p-type Cz-materials A, C, and D-1 as a function of the electron-to-hole concentrations *n/p*. The *Q* values were extracted from the slopes of the linear fits (solid lines; dashed lines indicate the experimental uncertainties) to the measurements for degradation under typical illumination conditions (room temperature, 0.1 suns) (a) after firing (filled symbols) and (b) after firing with subsequent industrial regeneration (open symbols). The extracted *Q* values do not change due to the regeneration within the measurement uncertainty.

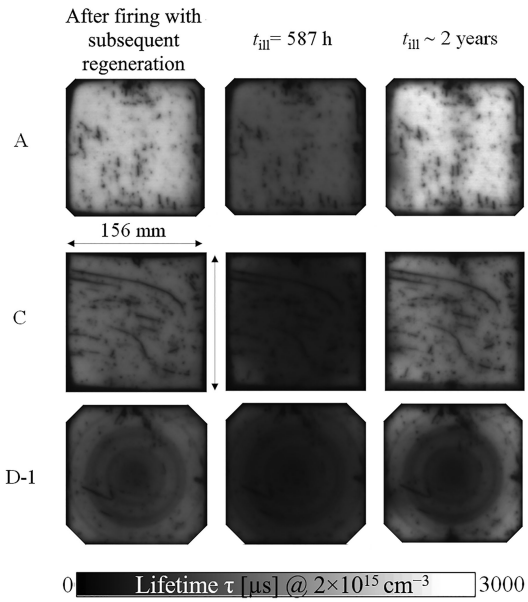

Fig. 3. PC-PLI measurements of materials A, C, and D-1 after firing with subsequent regeneration and different times of illumination near room temperature.

In order to extract further information regarding the properties of the activated defect in the regenerated samples, we analyze the injection-dependent lifetimes before and after degradation resulting in the lifetime of the activated defect $\tau_{\mathrm{def}} = (1/\tau_{\mathrm{deg}} - 1/\tau_0)^{-1}$. Plotting the normalized defect-related lifetime $\tau_{\mathrm{def}}/\tau_{\mathrm{n0}}$ versus the ratio of the electron-to-hole concentrations *n/p* can help to identify defect centers. The capture time constant τ_{n0} is determined graphically. According to [17] and [18], for a deep-level defect in p-type silicon the corresponding defect-related lifetime τ_{def} can be written as a linear function of *n/p*

$$\frac{\tau_{\mathrm{def}}}{\tau_{n0}} = 1 + Q\frac{n}{p} \tag{1}$$

where the slope is $Q = \tau_{\mathrm{p0}}/\tau_{\mathrm{n0}}$, and τ_{n0} and τ_{p0} are the capture time constants for electrons and holes, respectively, into the defect center.

As can be seen from Fig. 2, we determine the capture time constant ratio Q for the only-fired (filled symbols) samples as well as for the fired plus industrially regenerated lifetime samples (open symbols) to be in the range between 9 ± 3 and 12 ± 1. These values agree well with literature data for the BO defect, where Q values in the range between 10 and 12 have been reported [19]–[21]. Typically Q-values for the LeTID-specific defect are in the range between 20 and 36 [22]–[24] and can thus be excluded as degradation mechanism in our experiments. Our extracted Q values hence suggest that the regeneration process might not be completely finished during regeneration in the industrial belt furnace [25], [26]. However, the observed degradation kinetics slowed down significantly after regeneration. The detailed activation mechanism of the BO defect might hence have been changed by the regeneration treatment [27].

After complete degradation of the regenerated samples, the lifetime increases again with different time constants for the different materials. The lifetimes of the materials A–C increases back to their initial lifetimes within nearly two years of illumination near room temperature. These materials have a lower oxygen concentration of $(7–8) \times 10^{17}$ cm^{-3} than material D ($[O_i] \approx 10 \times 10^{17}$ cm^{-3}, see Table I). The lifetime of material D does not regenerate in the center within the time scale of our experiment. In a previous study of material C [16], we regenerated the fired samples of material C at 200 °C on a hotplate at 1 sun illumination intensity for several minutes. Subsequent room temperature illumination resulted in a lifetime degradation with a minimum reached only after 2000 h before recovery set in. It seems that the lifetime recovery was almost twice as fast as in our samples from material C, which were regenerated in the industrial belt furnace, possibly due to the increased regeneration temperature of 230 °C in the industrial regeneration furnace. We determine the rate constants of the defect deactivation R_{de} from the effective defect concentration $N_t^*(t)$ evolution by fitting an exponential decay function to the measured data. We experimentally determine $N_t^*(t) = 1/\tau_{\mathrm{ill}}(t) - 1/\tau_{\mathrm{0p}}$ from the measured τ_{0p} being the lifetime measured directly after regeneration in the industrial belt furnace and from τ_{ill} being the lifetime after long-term illumination for a period t near room temperature. All determined defect deactivation rates of materials A–C are in the same order of magnitude: $R_{\mathrm{de}}(\mathrm{A}) = 5 \times 10^{-4}$ h^{-1}, $R_{\mathrm{de}}(\mathrm{B}) = 7 \times 10^{-4}$ h^{-1}, and $R_{\mathrm{de}}(\mathrm{C}) = 3 \times 10^{-4}$ h^{-1}. In another experiment reported recently [28], lifetime samples made of 1–2 Ωcm boron-doped Cz-Si with the same passivation layers as applied in our present study, underwent a comparable RTA treatment at $\vartheta_{\mathrm{peak}} = 850$ °C with a belt speed of about 7.2 m/min in a DO-FF-8.600-300 belt furnace. In order to investigate the impact of the regeneration temperature, different temperatures were applied on a hotplate to regenerate the samples. At a regeneration temperature of 220 °C and an illumination intensity about 1 sun, the regeneration rate constant R_{de} was determined to be 144 h^{-1} [28]. The resulting Arrhenius plot of the determined regeneration rate constants for a regeneration temperature range between 80 and 220 °C [28] can be extrapolated to 30 °C, resulting in a range of regeneration rate constants between 0.03 to 0.0002 h^{-1}. This range fits with the regeneration rates of the present study (0.0003–0.0007 h^{-1}), determined near room temperature (30 °C) at an illumination intensity of 0.1 suns after firing with subsequent regeneration in an industrial belt furnace. However, the samples in this study are just illuminated by 0.1 suns instead of 1 sun. Therefore, the regeneration after firing with subsequent regeneration is much faster than expected.

Our experimental results could suggest that the light-induced defect activation and subsequent permanent deactivation might be explained by an incomplete regeneration process and that a certain fraction of BO defects might remain after regeneration. This would imply that during the industrial regeneration process, a part of the BO defects might be transformed into the in-active state, which can then lead to a re-degradation during subsequent illumination. Since the extracted degradation and regeneration rate constants after industrial regeneration do not correspond to the typical BO degradation and regeneration rate constants on non-regenerated Cz-Si wafers, the detailed defect kinetics has obviously changed significantly during the regeneration step. Current defect models [3], [21], [29] are not able to explain this behavior. Hence, an extension of current BO defect models seems to be necessary, which is, however, well beyond the scope of this study.

Fig. 3 shows PC-PLI measurements of the fired and subsequently regenerated Cz-Si materials A, C, and D-1 for three different times of illumination near room temperature. The left column shows lifetime images recorded directly after firing with subsequent regeneration, the middle column after 587 h of illumination and the right column after nearly two years of illumination. Materials A and B (B not shown here, because it shows exactly the same behavior as A) degrade slightly and homogeneously over the complete wafer area. Material C degrades more severely. The corners of the wafer, however, degrade slightly less, presumably due to the lower oxygen concentration compared to the center.

However, after nearly two years of illumination, material C shows a homogeneous lifetime distribution again. Moreover, material D already starts with an inhomogeneous lifetime distribution with ring-like defect structures right after regeneration (see Fig. 3, bottom row), which is frequently occurring in the seed end Cz-Si crystals [30] due to the Czochralski growth method. The lifetime of material D decreases over the complete

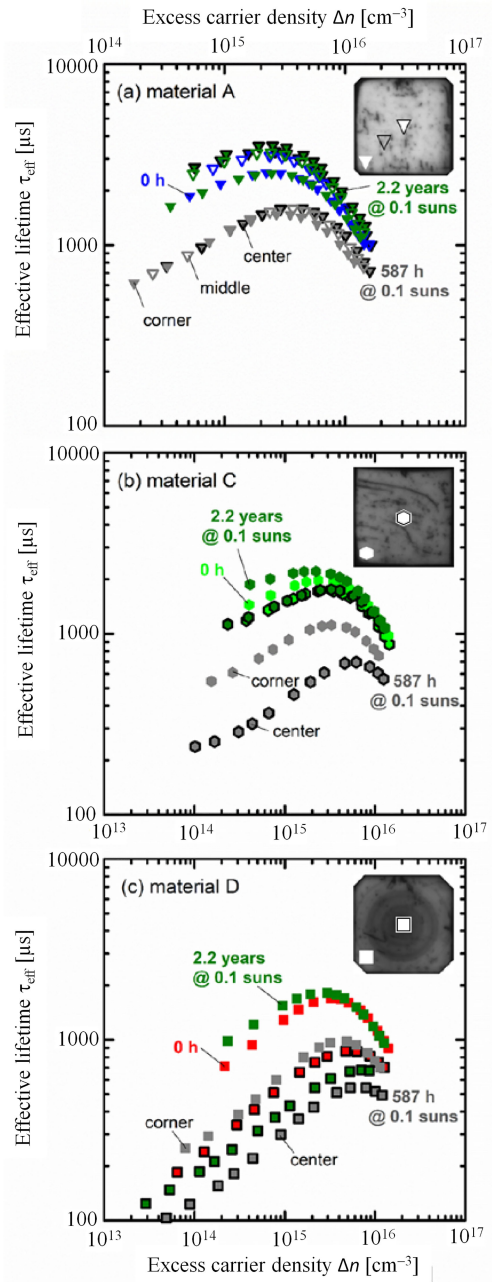

Fig. 4. Injection-dependent lifetime measurements at different locations from PC-PLI measurements for the materials (a) A, (b) C, and (c) D-1 after firing with subsequent regeneration in an industrial conveyor-belt furnace (0 h) and after 587 h as well as 2.2 years of illumination at room temperature after regeneration. Black framed symbols correspond to the center, whereas full and open symbols correspond to corner and middle position, respectively. (For interpretation of the references to color in this figure legend, the reader is referred to the web version of this article.)

wafer, but only the corners reach the initial lifetime again after 2.2 years of illumination.

Fig. 4 shows injection-dependent lifetimes extracted from the PC-PLI measurements at different locations on the wafers for different illumination times. Whereas for material A, the injection-dependent lifetime curves at the different wafer locations are practically identical, we observe strong differences for material C. For material C, the lifetime in the corner is significantly larger than the center region after 587 h of illumination. For example, at $\Delta n = 1 \times 10^{15}$ cm^{-3}, a lifetime of 920 µs is measured in the corner of the sample and a lifetime of 460 µs in the center. Only after 2.2 years of illumination, the lifetime curves coincide again. For material D, we observe already very different injection-dependent lifetime curves in the center and at the edge directly after regeneration. This suggests that the lifetime in these regions is limited by other recombination centers than the BO defect.

After 2.2 years of illumination, the lifetime curves measured in the corners of material D-1 coincide again, whereas we observe no lifetime regeneration in the center, which is limited by other background defects. An explanation for the different regeneration behavior in the center and in the corner of material D-1 could be the different oxygen concentrations [31].

IV. Conclusion

In this study, we have unambiguously demonstrated the benefits of adding an inline regeneration step to lifetime samples which underwent an industrial cell process sequence. The carrier lifetime evolution of the state-of-the-art boron-doped Cz-Si materials as well as material stemming from the seed end of a crystal were examined at room temperature under 0.1 suns illumination intensity up to 2.2 years after regeneration. Despite very high lifetimes measured directly after regeneration, we observed a subsequent renewed light-induced degradation in all materials, although up to 72% reduced at a much lower degradation rate (up to two orders of magnitude lower) compared to the standard BO degradation. The activated defect was found to have a capture time constant ratio Q in the range 9.5 ± 3.5 for all examined materials, which is comparable to the reported Q range for the BO defect. Hence, our results suggest that a fraction of BO was not fully removed by the fast industrial regeneration treatment. Due to the slower re-activation of the BO defect, the detailed degradation kinetics has, however, changed significantly, which is not explained by existing defect models. Since the observations are due to BO, in the context of the four-state model [27], any reverse reaction from state D to state A would be one possibility for degradation to occur during subsequent long-term light soaking. However, more work is required to fully understand the degradation observed in the present manuscript. On the long term, we observed a second regeneration process during illumination near room temperature, which saturated after two years, except for the material stemming from the seed end of the crystal, which was dominated by other background defects. This material also showed ring-like defect structures, which the other three materials did not show. The three state-of-the-art Cz-Si materials showed high lifetimes above 1 ms after more than two years of light exposure.

Acknowledgment

The authors would like to thank Olaf Romer for his support concerning the processing of the samples in an industrial belt furnace, Michael Winter for helping with the Q analysis and the State of Lower Saxony as well as the German Federal Ministry of Economics and Energy (BMWi). The content is the responsibility of the authors.

REFERENCES

[1] J. Schmidt, A. G. Aberle, and R. Hezel, "Investigation of carrier lifetime instabilities in Cz-grown silicon," in *Proc. 26th IEEE Photovoltaic Specialists Conf.*, Anaheim, CA, USA, 1997, pp. 13–18.

[2] J. Schmidt and K. Bothe, "Structure and transformation of the metastable boron- and oxygen-related defect center in crystalline silicon," *Phys. Rev. B*, vol. 69, no. 2, 2004, Art. no. 3302.

[3] T. Niewelt, J. Schon, W. Warta, S. W. Glunz, and M. C. Schubert, "Degradation of crystalline silicon due to boron–oxygen defects," *IEEE J. Photovolt.*, vol. 7, no. 1, pp. 383–398, 2017.

[4] A. Herguth, G. Schubert, M. Kaes, and G. Hahn, "Avoiding boron-oxygen related degradation in highly doped Cz silicon," in *Proc. 21st Eur. Photovolt. Solar Energy Conf.*, Dresden, Germany, 2006, pp. 530–537.

[5] V. Steckenreiter, D. C. Walter, and J. Schmidt, "Kinetics of the permanent deactivation of the boron-oxygen complex in crystalline silicon as a function of illumination intensity," *AIP Adv.*, vol. 7, no. 3, 2017, Art. no. 35305.

[6] D. C. Walter, B. Lim, K. Bothe, V. V. Voronkov, R. Falster, and J. Schmidt, "Effect of rapid thermal annealing on recombination centres in boron-doped Czochralski-grown silicon," *Appl. Phys. Lett.*, vol. 104, no. 4, 2014, Art. no. 042111.

[7] F. Fertig *et al.*, "Mass production of p-type Cz silicon solar cells approaching average stable conversion efficiencies of 22%," *Energy Procedia*, vol. 124, no. 13, pp. 338–345, 2017.

[8] B. Vicari Stefani *et al.*, "Large-area boron-doped 1.6 Ω cm p-type Czochralski silicon heterojunction solar cells with a stable open-circuit voltage of 736 mV and efficiency of 22.0%," *Sol. RRL*, vol. 4, no. 9, 2020, Art. no. 2000134.

[9] C. Derricks, A. Herguth, G. Hahn, O. Romer, and T. Pernau, "Industrially applicable mitigation of BO-LID in Cz-Si PERC-type solar cells within a coupled fast firing and halogen lamp based belt-line regenerator – A parameter study," *Sol. Energy Mater. Sol. Cells*, vol. 195, pp. 358–366, 2019.

[10] D. C. Walter, V. Steckenreiter, L. Helmich, T. Pernau, and J. Schmidt, "Production-compatible regeneration of boron-doped Czochralski-silicon in a combined fast-firing and regeneration belt-line furnace," in *Proc. 33rd Eur. Photovoltaic Sol. Energy Conf.*, Amsterdam, The Netherlands, 2017, pp. 377–381.

[11] R. A. Sinton and A. Cuevas, "Contactless determination of current–voltage characteristics and minority-carrier lifetimes in semiconductors from quasi-steady-state photoconductance data," *Appl. Phys. Lett.*, vol. 69, no. 17, pp. 2510–2512, 1996.

[12] K. R. McIntosh and R. A. Sinton, "Uncertainty in photoconductance lifetime measurements that use an inductive-coil detector," in *Proc. 23rd Eur. Photovoltaic Sol. Energy Conf.*, Valencia, Spain, 2008.

[13] S. Herlufsen, J. Schmidt, D. Hinken, K. Bothe, and R. Brendel, "Photoconductance-calibrated photoluminescence lifetime imaging of crystalline silicon," *Phys. Status Solidi*, vol. 2, no. 6, pp. 245–247, 2008.

[14] K. Bothe and J. Schmidt, "Electronically activated boron-oxygen-related recombination centers in crystalline silicon," *J. Appl. Phys.*, vol. 99, no. 1, 2006, Art. no. 13701.

[15] D. Sperber, A. Graf, D. Skorka, A. Herguth, and G. Hahn, "Degradation of surface passivation on crystalline silicon and its impact on light-induced degradation experiments," *IEEE J. Photovolt.*, vol. 7, no. 6, pp. 1627–1634, Nov. 2017.

[16] D. C. Walter, B. Lim, V. V. Voronkov, R. Falster, and J. Schmidt, "Investigation of the lifetime stability after regeneration in boron-doped Cz silicon," in *Proc. 29th EUPVSEC*, Amsterdam, The Netherlands, 2014, pp. 555–559.

[17] J. D. Murphy, K. Bothe, R. Krain, V. V. Voronkov, and R. J. Falster, "Parameterisation of injection-dependent lifetime measurements in semiconductors in terms of Shockley-Read-Hall statistics: An application to oxide precipitates in silicon," *J. Appl. Phys.*, vol. 111, no. 11, pp. 113709–1–113709–10, 2012.

[18] V. V. Voronkov, R. Falster, K. Bothe, B. Lim, and J. Schmidt, "Lifetime-degrading boron-oxygen centres in p-type and n-type compensated silicon," *J. Appl. Phys.*, vol. 110, no. 6, 2011, Art. no. 63515.

[19] J. Schmidt and A. Cuevas, "Electronic properties of the recombination centers responsible for the light-induced carrier lifetime degradation in boron-doped Czochralski silicon," *J. Appl. Phys.*, vol. 86, no. 6, 1999, Art. no. 3175.

[20] S. Rein and S. W. Glunz, "Electronic properties of the metastable defect in boron-doped Czochralski silicon: Unambiguous determination by advanced lifetime spectroscopy," *Appl. Phys. Lett.*, vol. 82, no. 7, pp. 1054–1056, 2003.

[21] J. Schmidt, K. Bothe, V. V. Voronkov, and R. Falster, "Fast and slow stages of lifetime degradation by boron–oxygen centers in crystalline silicon," *Phys. Status Solidi B*, vol. 116, 2019, Art. no. 1900167.

[22] D. Bredemeier, D. Walter, S. Herlufsen, and J. Schmidt, "Understanding the light-induced lifetime degradation and regeneration in multicrystalline silicon," *Energy Procedia*, vol. 92, pp. 773–778, 2016.

[23] A. E. Morishige *et al.*, "Lifetime spectroscopy investigation of light-induced degradation in p-type multicrystalline silicon PERC," *IEEE J. Photovolt.*, vol. 6, no. 6, pp. 1466–1472, Nov. 2016.

[24] M. Winter, D. Walter, D. Bredemeier, and J. Schmidt, "Light-induced lifetime degradation effects at elevated temperature in Czochralski-grown silicon beyond boron-oxygen-related degradation," *Sol. Energy Mater. Sol. Cells*, vol. 201, 2019, Art. no. 110060.

[25] G. Hahn, S. Wilking, and A. Herguth, "BO-related defects: Overcoming bulk lifetime degradation in crystalline Si by regeneration," *SSP*, vol. 242, pp. 80–89, 2015.

[26] S. Wilking, M. Forster, A. Herguth, and G. Hahn, "From simulation to experiment: Understanding BO-regeneration kinetics," *Sol. Energy Mater. Sol. Cells*, vol. 142, pp. 87–91, 2015.

[27] N. Nampalli *et al.*, "Multiple pathways for permanent deactivation of boron-oxygen defects in p-type silicon," *Sol. Energy Mater. Sol. Cells*, vol. 173, pp. 12–17, 2017.

[28] D. C. Walter, B. Lim, K. Bothe, R. Falster, V. V. Voronkov, and J. Schmidt, "Lifetimes exceeding 1 ms in 1-Ω cm boron-doped Cz-silicon," *Sol. Energy Mater. Sol. Cells*, vol. 131, pp. 51–57, 2014.

[29] A. Herguth and G. Hahn, "Kinetics of the boron-oxygen related defect in theory and experiment," *J. Appl. Phys.*, vol. 108, no. 11, 2010, Art. no. 114509.

[30] J. Haunschild, I. E. Reis, J. Geilker, and S. Rein, "Detecting efficiency-limiting defects in Czochralski-grown silicon wafers in solar cell production using photoluminescence imaging," *Phys. Status Solidi RRL*, vol. 5, no. 5–6, pp. 199–201, 2011.

[31] S. Wilking, S. Ebert, C. Beckh, A. Herguth, and G. Hahn, "Of Apples and Oranges: Why comparing BO regeneration rates requires injection level correction," in *Proc. 32nd Eur. Photovolt. Solar Energy Conf. Exhib.*, Munich, Germany, 2016, pp. 487–494.